nature biotechnology

ARTICLES

Neural subtype specification of fertilization and nuclear transfer embryonic stem cells and application in parkinsonian mice

Tiziano Barberi[1,2], Peter Klivenyi[3], Noel Y Calingasan[3], Hyojin Lee[1], Hibiki Kawamata[3], Kathleen Loonam[1], Anselme L Perrier[1], Juan Bruses[4], Maria E Rubio[5], Norbert Topf[6], Viviane Tabar[1], Neil L Harrison[6], M Flint Beal[3], Malcolm A S Moore[2] & Lorenz Studer[1]

Existing protocols for the neural differentiation of mouse embryonic stem (ES) cells require extended *in vitro* culture, yield variable differentiation results or are limited to the generation of selected neural subtypes. Here we provide a set of coculture conditions that allows rapid and efficient derivation of most central nervous system phenotypes. The fate of both fertilization- and nuclear transfer–derived ES (ntES) cells was directed selectively into neural stem cells, astrocytes, oligodendrocytes or neurons. Specific differentiation into γ-aminobutyric acid (GABA), dopamine, serotonin or motor neurons was achieved by defining conditions to induce forebrain, midbrain, hindbrain and spinal cord identity. Neuronal function of ES cell–derived dopaminergic neurons was shown *in vitro* by electron microscopy, measurement of neurotransmitter release and intracellular recording. Furthermore, transplantation of ES and ntES cell–derived dopaminergic neurons corrected the phenotype of a mouse model of Parkinson disease, demonstrating an *in vivo* application of therapeutic cloning in neural disease.

The differentiation of ES cells provides access to the earliest stages of development and may serve as a source of specialized cells for regenerative medicine. Several *in vitro* systems allowing derivation of neural progeny from ES cells have been described[1–4]. However, these differentiation protocols are hampered by disadvantages, such as the need for extended *in vitro* culture[2,5,6], cell line– and strain-dependent variability of the differentiation results[2,7], low efficiency of neural induction[3,4] or generation of a limited number of neural subtypes[1].

Here we describe a coculture-based ES cell differentiation system that provides both fast, efficient neural induction and the ability to generate a wide range of neural subtypes, including clonally defined neural stem cells (NSCs). We also developed protocols for the selective generation of dopaminergic, serotonergic, cholinergic and GABAergic neurons, as well as astroglia and oligodendroglia.

Compared with earlier techniques, this system exhibited minimal variability in obtaining neural cells from a wide range of both fertilization- and ntES cell–derived cells, facilitating the use of ntES cell lines in therapeutic cloning in neural diseases. *In vivo* survival of ES cell–derived dopaminergic neurons[1] and correction of the phenotype in parkinsonian rats using ES cells overexpressing Nurr1 (ref. 8) have been described. However, the therapeutic potential of ntES cells and of ES cells not overexpressing Nurr1 has not been demonstrated. Here we show that transplantation of naive ES and ntES cell–derived dopa-minergic neurons into parkinsonian mice resulted in the long-term survival of the transplanted dopaminergic neurons and the correction of behavioral deficits.

RESULTS

Neural induction of mouse ES cells

We induced neural differentiation by coculturing ES cells with murine bone marrow–derived stromal feeder cell lines MS5 (ref. 9) and S17 (ref. 10) or with primary stromal feeder cells obtained from the aorta-gonad-mesonephros (AGM) region. Stromal feeder cell lines such as MS5 are preadipocytic mesenchymal cells that were originally developed to support *in vitro* growth and long-term expansion of highly purified hematopoietic stem cells. We seeded undifferentiated mouse ES cells on stromal cells at low density, and induced neural differentiation in serum replacement medium (SRM). Within 3 d, ES cell–derived cells had formed small epithelial structures (Fig. 1a), and by day 6, virtually all ES cell–derived colonies were immunoreactive to neural precursor markers such as nestin[11] (Fig. 1b), neural cell adhesion molecules (NCAMs) and musashi[12]. Subsequent culture in N2 medium supplemented with basic fibroblast growth factor (bFGF)[13,14] allowed the purification and propagation of neural precursor cells. Neuronal differentiation was induced by bFGF withdrawal and addition of ascorbic acid[2,15]. We monitored *in vitro* progression of ES cell

[1]Laboratory of Stem Cell and Tumor Biology, Division of Neurosurgery and Developmental Biology Program. [2]James Ewing Laboratory for Developmental Hematopoiesis, Cell Biology Program, Sloan-Kettering Institute. [3]Department of Neurology and Neuroscience, Weill Medical College of Cornell University, New York, New York 10021, USA. [4]Laboratory of Neural Development, Cellular Biochemistry and Biophysics Program, Sloan-Kettering Institute, 1275 York Avenue, New York, New York 10021, USA. [5]Department of Physiology and Neurobiology, The University of Connecticut, Storrs, Connecticut 06269, USA. [6]Departments of Anesthesiology and Pharmacology, Weill Medical College of Cornell University, New York, New York 10021, USA. Correspondence should be addressed to L.S. (studerl@mskcc.org).

Published online 21 September 2003; doi:10.1038/nbt870

ventral neuronal subtypes, such as dopamine neurons. Exposure to retinoic acid, FGF4, FGF8, or bFGF led to enrichment of cholinergic, serotonergic, dopaminergic and GABAergic neurons, respectively. The selective generation of these neuronal subtypes was correlated with the increased expression of spinal cord (cholinergic), hindbrain-midbrain (ser-otonergic, dopaminergic) and forebrain (GABAergic) markers. The specific conditions for dopamine neurons were: days 0–5, SRM; days 5–8, SRM + FGF8 + SHH); days 8–11, N2 medium (N2) + bFGF + FGF8 + SHH; days 11–14, N2 + ascorbic acid + brain-derived neurotrophic factor (BDNF). Conditions for serotonin neurons were the same as those for dopamine neurons, except on days 5–8 (SRM + FGF4 + SHH). Conditions for motor neurons were: on days 0–4, SRM; days 4–8, SRM + SHH + retinoic acid; days 8–11, N2 + bFGF + SHH; days 11–14, N2 + ascorbic acid + BDNF. Conditions for GABAergic neurons were: days 0–5, SRM; days 5–9, N2 + bFGF; days 9–11, N2 + bFGF + SHH + FGF8; days 11–14, N2 + BDNF + NT4. Forebrain identity of GABAergic neurons was demonstrated using BF1/lacZ knock-in reporter ES cells (Fig. 3e). The winged-helix transcription factor brain factor-1 (BF1; also called foxg1) is a forebrain-specific marker within the CNS[16]. The MS5 GABA protocol caused a marked induction of BF1 expression, as assessed by β-gal histochemistry of the ES cell–derived progeny, consistent with forebrain-specific differentiation. A schematic representation of all neural subtype–selective protocols is provided as Figure 4.

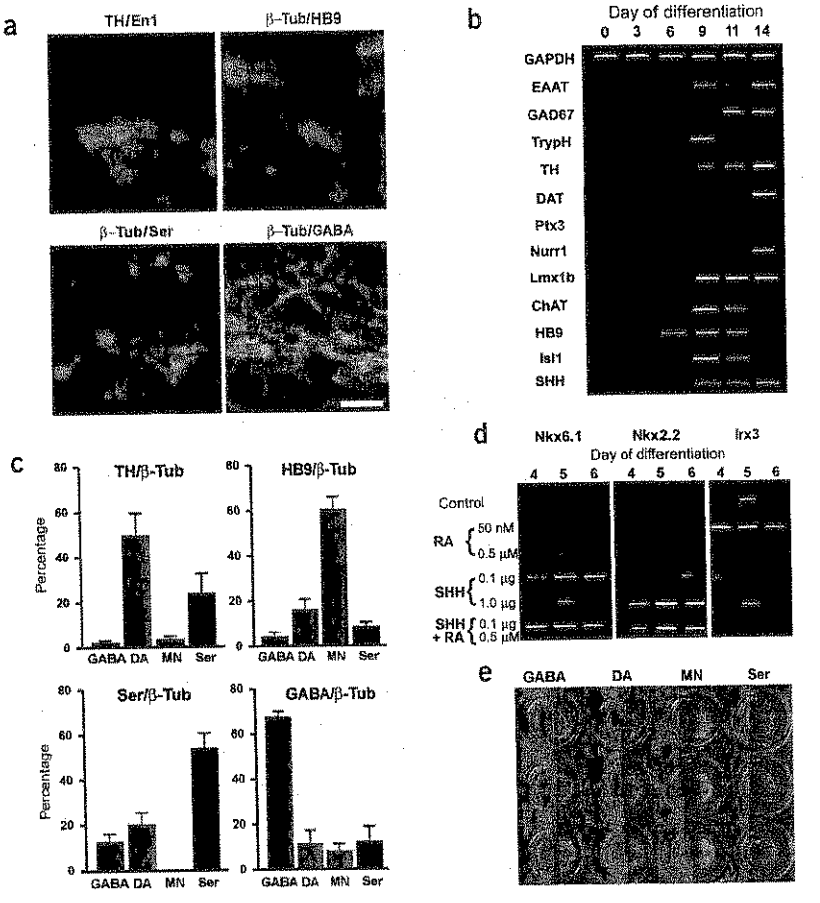

Figure 3 Neuronal fate specification. (**a**) Immunocytochemistry for neuron subtype-specific markers under conditions that enrich for midbrain dopamine (DA) neurons (TH/En1), motor neurons (MNs; β-Tub/HB9), serotonin neurons (β-Tub/Ser) and GABA neurons (β-Tub/GABA). Scale bar, 20 μm for all panels. (**b**) RT-PCR analysis of neurotransmitter and other subtype-specific markers confirms the presence of multiple neuronal subtypes such as GABA, serotonin, midbrain DA and MNs after 6–9 d of *in vitro* differentiation. (**c**) Percentage of β-tubulin$^+$ neurons expressing DA, MN, serotonin or GABA markers under induction protocols optimized for each neuronal subtype. Each subtype-specific condition resulted in a significant increase for a given phenotype ($^*P < 0.05$ against each other group; ANOVA: Scheffé). (**d**) Effect of SHH and retinoic acid (RA) on induction of the transcription factors Nkx6.1, Nkx2.2 and Irx3 during MS5-induced *in vitro* differentiation. RA and SHH were added on days 3–7. (**e**) X-gal cytochemistry of BF1-lacZ knock-in ES cells differentiated under conditions selective for GABA, DA, MN and serotonin neurons. Data show a marked increase in forebrain differentiation under GABA-selective conditions.

These protocols for glial and neuronal subtype-specific differentiation yielded comparable results in a variety of ES (CJ7, A2.2, E14, B5) and ntES (C15, C16, CT1, CT2, CN1, CN2) cell lines. Head-to-head comparison of the MS5 with the multistep embryoid body–based dopamine neuron differentiation protocol[2,7] confirmed reduced variability and increased yield of TH-expressing (TH$^+$) neurons for both ES and ntES cell lines (Fig. 5a). Cloned ES cell lines were derived through nuclear transfer from adult tail tip or cumulus cells as described[7]. Highly reproducible differentiation among all ES and ntES cell lines tested was a surprising finding, given earlier results with embryoid body–based protocols[7].

Functional characterization of ES cell–derived neurons *in vitro*

A definite marker of neuronal fate is the generation of synapses. ES cell–derived neurons frequently contained aggregates of synaptic vesicles (50–100 nm) in the vicinity of the cell membrane (Fig. 5b, left). In addition, we detected larger (>100 nm), electron-dense vesicles resembling those observed at dopamine terminals. Synaptic contacts (Fig. 5b, right) were seen between dendritic and axonal processes, or between an axonal process and a cell body. In addition to ultrastructural evidence of synapse formation, HPLC revealed that ES cell–derived dopamine neurons released dopamine both basally and upon stimulation with KCl (Fig. 5c). Electrophysiological properties of ES cell–derived neurons were assessed in single-cell recordings (Fig. 5d). ES (B5) and ntES (CT2) cells constitutively expressing enhanced green fluorescent protein (eGFP) were differentiated using the MS5 protocol for dopamine neuron differentiation and were replated on glass coverslips at day 12 of differentiation. Cells were kept in N2 medium supplemented with ascorbic acid and BDNF for recordings at days 16–20 of differentiation. Depolarization-induced action potentials that could be reversibly blocked by tetrodotoxin (TTX) were observed in 54% of all ES cell–derived ($n = 24$) and two out of two (100%) ntES cell–derived cells

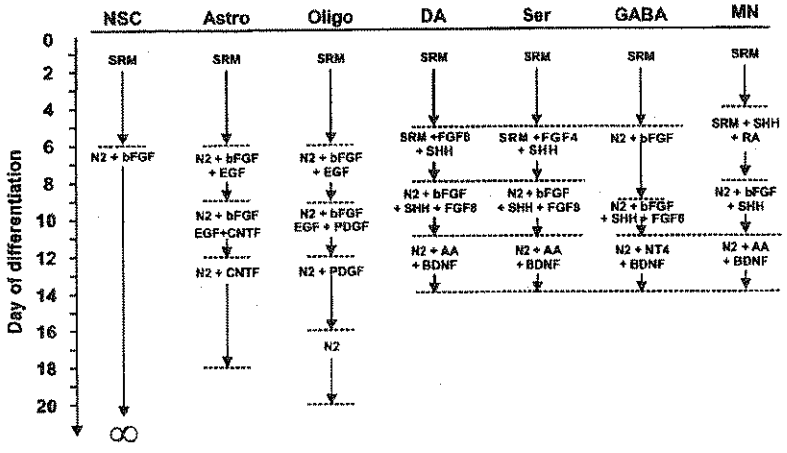

Figure 4 Schematic representation of culture conditions. The temporal sequence of medium and growth factors is listed for the derivation of specific neural subtypes from mouse ES and ntES cells. See Methods for detailed technical information. Astro, astrocytes; DA, dopamine neurons; GABA, GABA neurons; MN, motor neurons; NSC, neural stem cells; Oligo, oligodendrocytes; Ser, serotonin neurons.

(Fig. 5d). These data confirm that MS5-induced ES cell differentiation leads to rapid development into functional neurons.

Transplantation into parkinsonian mice

The *in vivo* function and therapeutic potential of MS5-induced ES cell–derived neuronal subtypes were assessed in mice with 6-hydroxydopamine (6-OHDA)-induced lesions. Unilateral lesions were established by intraventricular 6-OHDA injections, which resulted in the loss of 69.4 ± 7.6% of the midbrain dopamine neurons 8 weeks after the injections (n = 5). ES cells were differentiated on MS5 for 11 d under dopamine neuron–enriching conditions, replated in the absence of feeders and grown for an additional 3–4 d in N2 medium supplemented with BDNF and ascorbic acid. Cells (10^5 cells derived from eGFP-expressing ES (B5) or ntES (CT2) cell lines) were harvested by mechanical removal and subsequently injected into the ipsilateral striatum (n = 6 mice for each cell line and for saline-injected controls). Histological analyses done 2 months after transplantation showed grafts that extended over a large portion (up to 10 mm^3, as assessed by Cavalieri estimator) of the host striatum (Fig. 6a–c). However, within this volume, areas of grafted cells were typically interspersed with the striatum, precluding an accurate measure of total graft volume. The highest density of TH^+ cells was found at the interface of grafted and host cells. Notably, the location of grafted $eGFP^+$ cells was largely restricted to the striatum without crossing into the neighboring cortex (Fig. 6d). Coexpression of the DAT and aromatic acid decarboxylase (AADC) (Fig. 6e,f) confirmed dopamine neuron fates in ≥70% of all TH^+ cells in the graft. The proportion of TH^+ cells expressing dopamine-β hydroxylase, a marker of noradrenergic neurons, was <5%. Stereological counts yielded an average of 7,498 ± 2,338 TH^+ cells and 22,830 ± 8,451 TH^+ cells for B5 and CT2 cells, respectively (Fig. 6g). No TH^+ cells were detected in the striata of control, saline-injected mice. *In vivo* graft function was assessed by reversal of amphetamine- and apomorphine-induced rotation behavior (Fig. 6h,i). All mice grafted with ES or ntES cell–derived cells showed >70% reduction in both amphetamine and apomorphine scores (n = 6 in each group). No reductions in either score were observed in control mice (n = 6; Fig. 6h,i). These data demonstrate robust alleviation of the behavioral deficits in grafted mice. Notably, no overcompensation (negative rotations after amphetamine challenge) was observed, as reported earlier for Nurr1-overexpressing ES cells[8]. This result was surprising because some mice had >40,000 surviving TH^+ cells in the striatum, a number that exceeds the ~10,000 midbrain dopamine neurons present in the adult mouse midbrain.

Whereas ntES cell grafts appeared larger in size than ES cell grafts, in accordance with the increased number of TH^+ neurons (Fig. 6g), no obvious differences in fiber outgrowth or neural subtype composition was detected. The extent of TH^+ fiber outgrowth was not assessed across multiple sections, but within a single section (50 µm thickness) TH^+ fibers could be traced for as far as 400 µm into the host striatum (see **Supplementary Fig. 3** online). Grafts typically contained a few GABAergic, cholinergic and serotonergic neurons in addition to the TH^+ cell population (**Supplementary Fig. 3**). Immunohistochemistry for CD40 (activated immune cells), CD11b (microglia) and GFAP (astrocytes) detected no obvious signs of inflammation or immune response against the grafted cells (**Supplementary Fig. 3**). No signs of aberrant differentiation or teratocarcinoma formation were observed on routine hematoxylin and eosin staining and examination. The only significant difference between ntES and ES cell grafts was an increased TH^+ soma size, as assessed by stereological measures (nucleator probe): ntES dopamine neurons (n = 244), 2,268 ± 129 μm^3; ES dopamine neurons (n = 168), 3,088 ± 126 μm^3; $P < 0.001$.

DISCUSSION

In the present study, we describe a fast and efficient method for the *in vitro* neural conversion of mouse ES cells. We and others have reported elsewhere the generation of neural progeny from a variety of pluripotent cell sources[1,2,7,8,17,18]. The protocols described here offer a simpler, more rapid and versatile platform for the selective generation of a wide range of neural phenotypes. *In vitro* induction of region-specific fates has been reported in embryoid body–based culture systems, including the generation of midbrain dopamine neurons[2], hindbrain serotonin neurons[8] and hindbrain–spinal cord motor neurons[19]. We expand on these findings by demonstrating the efficient and selective generation of all these phenotypes in a single feeder-based system. In addition, we demonstrate the selective generation of forebrain GABAergic neurons from ES cells, which has not been reported before.

Whereas initial data suggested that stromal feeder cells induce midbrain neuronal fates by default, our study demonstrates that regional fate specification can be controlled by manipulation of external medium conditions and by sequential patterning cues that seem to recapitulate *in vivo* development (see **Supplementary Fig. 1** online). Studies in *Xenopus laevis* have suggested that the early neural fate is anterior in nature by default[20] but modulated and posteriorized by retinoid, FGF and Wnt signaling[21]. Our data are compatible with this proposal, considering that the chief modification for generating anterior fates consisted of a delayed application of FGF8 and SHH, after the time window during which *in vitro* specifications of midbrain-hindbrain organizer genes typically occur (Fig. 3b). Similarly, an early switch to N2 medium + bFGF was chosen to prevent the midbrain-promoting activity of SRM[1] and to keep early neural precursors under

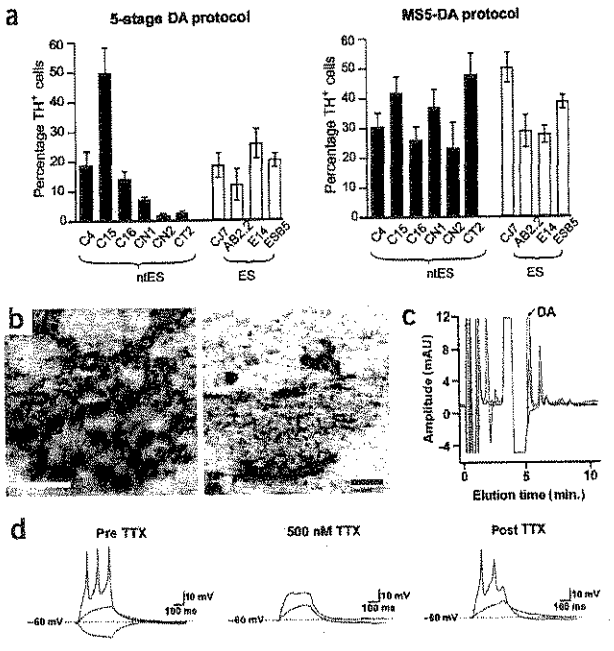

Figure 5 Variability of dopamine (DA) neuron differentiation and *in vitro* function of ES cell–derived neurons. (**a**) The percentage of TH$^+$ neurons derived from various ES and ntES cell lines differentiated with the MS5 or the embryoid body–based DA neuron protocol. In addition to decreased variability, there was a significantly increased percentage of TH$^+$ cells ($P < 0.001$, ANOVA: Scheffé). (**b**) Electron microscopy shows numerous boutons filled with synaptic vesicles (left). These structures often made axodendritic and axosomatic contacts and displayed pre- and postsynaptic densities (right). (**c**) Example of an HPLC chromatogram showing high levels of DA in the medium of ES cell–derived neurons (green line, medium conditioned for 24 h: 522 ± 124 pg/ml). Relatively low basal DA release was detected (blue line, exposure to buffer for 15 min: 68 ± 34 pg/ml) as compared with very high levels of DA after 15 min of KCl-evoked depolarization (red line, 1,398 ± 322 pg/ml). (**d**) ES cell–derived neurons were patched in the whole-cell configuration in current-clamp mode. Action potentials were evoked by depolarizing currents at a threshold of –40 mV. All action potentials were TTX sensitive. Scale bars in **b**, 0.12 µm.

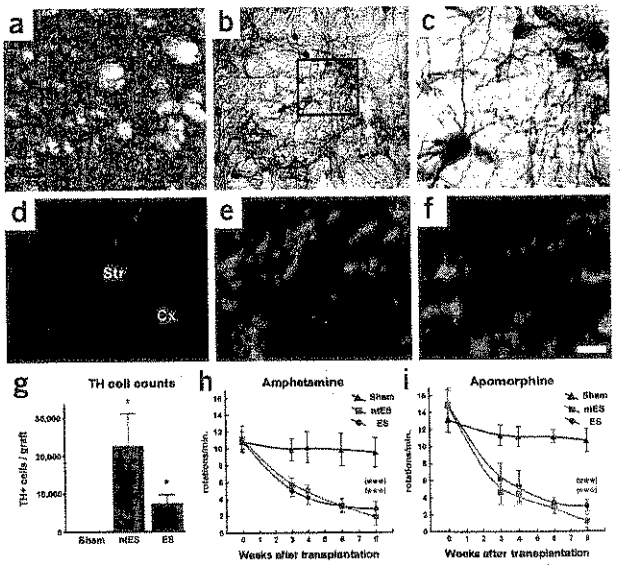

Figure 6 *In vivo* function of ES cell–derived neurons. (**a–c**) TH immunohistochemistry of the striatum in a mouse grafted with ntES cell–derived cells. (**a**) TH$^+$ fibers in the striatum contralateral to the lesion. (**b**) TH$^+$ cells and fibers within the graft. (**c**) High-power image of boxed area in **b** shows large TH$^+$ cells with complex neuritic arborizations. (**d**) GFP$^+$ grafted cells were confined to the striatum (Str) and did not cross into cortical areas (Cx). (**e,f**) Double immunohistochemistry for TH (green) and DAT (red) in **e** and TH (green) and AADC (red) in **f** show colocalization (yellow) in the majority of TH$^+$ cells. (**g**) Number of surviving TH$^+$ cells in the graft. Data are mean ± s.d., $P < 0.05$ for both ES and ntES compared with sham group (ANOVA: Scheffé). (**h, i**) Amphetamine- and apomorphine-induced rotation in ES, ntES and sham-grafted mice. Data are mean ± s.d., $P < 0.001$ for both ES and ntES compared with sham group (ANOVA interaction: weeks after grafting × cell type). Scale bar in **f**, 100 µm for **a**, **b**, **d**; 50 µm for **e** and **f**; 25 µm for **c**.

proliferative conditions. Late application of SHH and FGF8 was initiated to mimic signaling within the basal forebrain essential for generating the ventral telencephalon (GABAergic neurons[22]). It thus appears that stromal feeder differentiation does not bias regional identity of ES cell–derived progeny and is responsive to developmentally based patterning strategies. The specificity of forebrain versus midbrain versus hindbrain versus spinal cord induction in our culture protocols provides an *in vitro* assay to screen for additional molecules involved in anteroposterior (AP) patterning.

In contrast to the PA6 feeder system, in which no significant glial differentiation was reported[1], our technique allows efficient and rapid differentiation into both astroglia and oligodendroglia. However, a direct comparison of MS5 and PA6 revealed that both systems can derive astroglial and oligodendroglial progeny under appropriate culture conditions (data not shown). Our study demonstrates neural-inducing activity in S17, in addition to MS5 and PA6, as well as in primary stromal cells derived from the AGM region, suggesting that the inducing activity is not a unique feature of bone marrow–derived stromal cells. Comparisons between various stromal cell types with native neural-inducing activity, neural-inducing activity upon paraformaldehyde crosslinking[1] or noninducing feeders should help identify the molecular nature of neural induction by stromal feeder cells.

Neural induction with the MS5 protocol was more robust than that involving embryoid body–based systems. This was reflected in our successful use here, in the treatment of parkinsonian mice, of the eGFP-expressing line CT2, which had the lowest efficiency of dopaminergic differentiation among all ntES cell lines in embryoid body–based protocols[7]. Efficient neural differentiation of a wide range of ntES cells is a prerequisite for future autologous applications in therapeutic cloning, in which it will be unrealistic to adapt culture conditions to every single ntES cell line. The efficiency of the culture system is further demonstrated by calculating the number of specialized progeny, such as dopamine neurons, obtained from a single ES cell. Whereas embryoid body–based protocols typically yield two to three dopaminergic neurons per ES cell initially plated[2], the MS5 dopamine protocol results in 1,000 dopaminergic neurons (1×10^3 ES cells yield an average of 2×10^6 TUJ1$^+$ neurons and 0.98×10^6 dopamine cells at day 14 of differentiation).

Our *in vitro* data add to the functional characterization of ES cell–derived neurons. Although electrophysiological evidence of synapse formation using embryoid body–based multistage differentiation protocols has already been reported[2], we provide proof that ntES

cell–derived neurons have the same functional properties. Therefore, cloning and long-term expansion of undifferentiated ntES cells do not interfere with the functionality of their differentiated progeny. The ultrastructural detection of typical large, dense-core vesicles suggests that these are dopaminergic neurons.

There has been great interest in developing renewable cell sources for the generation of dopamine neurons in the experimental treatment of Parkinson disease. Although some success has been reported in obtaining dopamine-like neurons *in vitro* from CNS-derived precursors, CNS-based sources of dopamine neurons generally showed limited *in vitro* expansion[14,23] and *in vivo* function[24,25]. Two recent studies using undifferentiated ES cells[26] or neurally induced ES cells overexpressing Nurr1 (ref. 8) have shown behavioral improvement in 6-OHDA-lesioned rats. However, undifferentiated ES cells caused teratomas in a large proportion of grafted animals[26]. No tumors were reported in grafts of dopamine neurons derived from Nurr1-overexpressing ES cells. However, the use of cells expressing transgenes raises questions about long-term safety. Our study demonstrates functionality of ES cell– and ntES cell–derived neurons in 6-OHDA-lesioned mice, without the requirement for exogenous Nurr1 expression. The transplantation results using ntES cell–derived dopamine neurons in parkinsonian mice demonstrates the efficacy of therapeutic cloning in an animal model of CNS disease. Earlier work has shown *in vivo* functionality of bovine dopamine neurons extracted from cloned fetuses[27]. However, the use of cloned fetuses as cell donors raises ethical barriers that preclude applications in human disease. Notably, the dopamine neuron survival rate *in vivo* was higher in ntES than in ES cell–derived grafts (~80% versus 40%, 8 weeks after transplantation). The presence of up to 40,000 surviving TH^+ neurons in some mice suggests that at least some of the ES cell–derived dopamine neurons were born *in vivo*.

Our differentiation method provides a means to efficiently direct ES and ntES cells into a wide variety of specific neural fates. Our results also demonstrate the potential of therapeutic cloning in mouse models of Parkinson disease and suggest additional applications for motoneuronal and demyelinating disorders. Future therapeutic applications may require extensive work to adapt our protocols to human ES cells.

METHODS

Cell culture. Data were obtained with CJ7, B5 and BF1/lacZ-73 ES cells[28], and C15 and CT2 ntES cells[7]. In addition, A2.2, E14 ES cells, and CT1, CN1, CN2 and C16 ntES cells[7] were used to compare the variability of neural differentiation among culture systems. Undifferentiated ES and ntES cells were maintained as described[29].

Stromal cells. The stromal cell lines successfully used in this study were MS5 (Kirin Brewery), S17 (provided by M. Moore), PA6 (Riken Cell Bank) and various (a total of 10) AGM-derived stromal cell lines. AGM stromal cells were established as reported[30]. All the stromal cell lines were maintained as monolayer cultures in α-minimal essential medium (α-MEM) containing 10% FBS and 2 mM L-glutamine (Gibco-Invitrogen) and were passaged at 70% confluency. For neural induction of ES cells, stromal cells were grown to 100% confluency (contact inhibition–induced growth arrest). Alternatively, stromal cells can be growth arrested by irradiation and replated at 50×10^3 cells/cm^2. Neural induction is initiated by plating undifferentiated ES cells as single-cell suspension at a density of 50 cells/cm^2 in SRM composed of Dulbecco's modified Eagle medium with 15% serum replacement, 2 mM L-glutamine and 10 μM β-mercaptoethanol (Gibco-Invitrogen).

Neural stem cells. ES cell–derived NSCs were generated after 6 d on MS5 coculture in SRM (changed every 2–3 d), gently trypsinized and replated at single-cell densities (~5–10 cells/cm^2 on polyornithine- and fibronectin-coated dishes in N2 medium[13] supplemented with 10 ng/ml bFGF. These ES cell–derived NSCs can be cloned and propagated under conditions identical to those described for primary rat NSCs[13].

Astrocytes. After 6 d of culture in SRM, ES cell–derived neural progenitors were induced to proliferate in N2 medium supplemented with 10 ng/ml bFGF and 20 ng/ml EGF (days 6–9), and then cultured for an additional 3 d in N2 medium with bFGF, EGF and 20 ng/ml CNTF. At day 12 all growth factors except CNTF were withdrawn, and cells were typically analyzed at day 18.

Oligodendrocytes. Conditions for oligodendroglial differentiation were identical to those for astrocytic differentiation until day 9. From day 9 to day 12, cells were exposed to N2 medium supplemented with 20 ng/ml PDGF in addition to bFGF and EGF. These immature oligoprogenitors were expanded in PDGF alone from day 12 to day 16 and differentiated by PDGF withdrawal. The addition of 10 ng/ml neurotrophin-3 and 40 ng/ml triiodothyronine (T3) can be used to enhance differentiation further.

Glial differentiation can be induced in the absence of stromal feeders after replating ES cell–derived neural precursors at day 6 of differentiation on MS5 as for NSCs (see earlier).

Dopamine neurons. After 5 d of culture, 200 ng/ml SHH and 100 ng/ml FGF8 were added to the SRM, and then the medium was changed to N2 supplemented with SHH and FGF8 in the presence of 10 ng/ml bFGF (days 8–11). At day 11, terminal differentiation was induced by withdrawal of SHH, FGF8 and bFGF and the addition of 200 μM ascorbic acid and 20 ng/ml BDNF.

Serotonin neurons. The same culture conditions were used as for dopamine neurons, except that 100 ng/ml FGF4 was added instead of FGF8 from day 5 to day 8.

GABA neurons. After 5 d in SRM, the cells were transferred to N2 medium supplemented with 10 ng/ml bFGF for 4 d. At day 9, 200 ng/ml SHH and 100 ng/ml FGF8 were added to the N2-bFGF for 2 d more. Differentiation was induced by mitogen withdrawal and the addition of 20 ng/ml neurotrophin-4 (NT4) and 20 ng/ml BDNF.

Motor neurons. At day 4 of culture, 500 ng/ml SHH and 1 μM retinoic acid were added to SRM, and then the cultured was transferred to N2 medium supplemented with 10 ng/ml bFGF and SHH from day 8 to day 11. Differentiation was induced at day 11 in N2 medium supplemented with ascorbic acid and 20 ng/ml BDNF. For long-term culture of motor neurons, the addition of 10 ng/ml glial-derived neurotrophic factor is required.

For culture of all neuronal subtypes in the absence of stromal feeders, ES cell–derived progeny can be removed at day 11 of differentiation, after incubation in Ca- and Mg-free Hanks balanced salt solution (HBSS) for 30 min, mechanical trituration and replating at 50×10^3 cells/cm^2.

All growth factors were purchased from R&D Systems; all-*trans* retinoic acid and T3 were from Sigma-Aldrich.

Immunohistochemistry. Cells were fixed in 4% paraformaldehyde–0.15% picric acid and were stained with the following primary antibodies. Rabbit polyclonal antibodies: against nestin no. 130 (provided by R. McKay); musashi, GFAP, HB9 (Chemicon); TH (PelFreez); GABA and serotonin (Sigma-Aldrich); β-tubulin III (Covance). Mouse monoclonal antibodies: against Tuj1 (Covance); MBP, NG2, O4 and O1 (Chemicon); CNP (Sternberger Monoclonals); NCAM (BD Pharmingen); TH (Sigma-Aldrich); En1, DSHB (provided by T. Jessell). Appropriate cyanin-2- (Cy2) and Cy3-labeled secondary antibodies (Jackson ImmunoResearch) and DAPI counterstain were used for visualization.

RT-PCR. Total RNA was extracted using Trizol ultra pure reagent (Gibco-Invitrogen) and subsequently incubated with DNA*free* (Ambion) to minimize genomic DNA contamination. SuperScript kit (Gibco-Invitrogen) was used for reverse transcription (5 μg RNA per condition). PCR conditions were optimized by varying the $MgCl_2$ concentration and cycle numbers to determine a linear amplification range. PCR products were identified by size and confirmed by DNA sequencing. Primer sequences, cycle numbers and annealing temperatures are provided as **Supplementary Table 1** online. Gels were imaged using a 12-bit CCD camera (Alphainnotech).

Electron microscopy. Cells differentiated for 11 d in dopamine neuron–promoting conditions were replated on eight-well Permanox chamber slides (Lab-Tek; Nunc) (1×10^5 cells/well), and were cultured for an additional 5–7 d before analysis. Cultures were fixed in 4% paraformaldehyde–2.5% glutaraldehyde, washed in cacodylic buffer, post-fixed in 1% osmium tetroxide, dehydrated in ethanol and propylene oxide, infiltrated and flat embedded in Epon resin. Ultrathin sections were stained with 1% uranyl acetate and 0.3% lead citrate and were observed with a Jeol 1200EX or a Zeiss 100CX II transmission electron microscope. Electron micrographs were taken at 50,000× magnification.

HPLC analysis. Dopamine release was measured by RP-HPLC, as described[31]. Briefly, samples were collected at day 14 of differentiation conditioned medium (24 h), basal release (15 min in HBSS) and evoked release (15 min in HBSS + 56 mM KCl). Samples were stabilized and extracted by aluminum adsorption (Chromosystems). Separation of injected samples (ESA Autosampler 540) was achieved by isocratic elution in MD-TM mobile phase (ESA) at 0.5 ml/min. The oxidative potential of the analytical cell (ESA Mod. 5011, Coulochem II) was set at 350 mV. Results were validated by coelution with catecholamine standards under varying buffer conditions and detector settings.

Electrophysiology. Cells were placed on the stage of an inverted microscope (Axiovert 25; Zeiss). The culture medium was replaced by a physiological saline solution containing 145 mM NaCl, 3 mM KCl, 1.5 mM $CaCl_2$, 1 mM $MgCl_2$, 5 mM glucose, 10 mM HEPES (pH 7.4) and having 320–330 mOsm osmolarity. GFP^+ cells were identified by fluorescence microscopy, and recordings were done at 25 °C, using the whole-cell patch-clamp technique. The patch pipette solution contained 135 mM potassium gluconate, 2 mM NaCl, 1 mM $CaCl_2$, 1 mM $MgCl_2$, 10 mM HEPES, 10 mM EGTA, 2 mM Mg-ATP, 0.4 mM Na-GTP (pH 7.3) and osmolarity adjusted to 295 mOsm. Pipette-to-bath resistance was typically 5–10 MΩ. When TTX was applied, the final concentration was 500 nM. Cells were recorded in current-clamp mode using the Axopatch 1C amplifier, and the membrane potential was manually adjusted to –60 mV. Current commands were applied for 300 ms using pCLAMP 5, and membrane potential was digitized with an analog-to-digital converter (TL-1 DMA interface) at 20 kHz. Data were analyzed using Axograph 4.6 (all from Axon Instruments).

***In vivo* studies.** Male 129Sv] mice (30–35 g; Jackson Laboratory) were housed and treated according to the National Institutes of Health (NIH) guidelines. All protocols were approved by the Institutional Animal Care and Use Committee of Sloan-Kettering Institute and Cornell University.

The mice were anesthetized with isoflurane, and 50 µg 6-OHDA (Sigma-Aldrich) diluted in 2 µl 0.05% ascorbic acid was injected into the lateral ventricle at the following coordinates (in millimeters): AP, 0.3 (from bregma); ML, 1.0; DV, 3.0 (from dura). To protect noradrenergic neurons, 30 min before 6-OHDA injection, desipramine (Sigma-Aldrich) was injected intraperitoneally (i.p.) at a dose of 25 mg/kg. Intraventricular 6-OHDA administration led to a complete denervation of the medial striatum with only a few remaining TH^+ fibers in the lateral striatum. Mice with successful lesions were selected, and 10^5 cells resuspended in 1 µl were injected into the striatum at the following coordinates (in mm): AP, 0.5; ML, 2.0; DV, 3.5.

Behavioral tests were done 4 weeks before transplantation and 3, 4, 6 and 8 weeks after grafting. Mice were injected i.p. with apomorphine (10 mg/kg; ref. 32) and, after a 2-d interval, with amphetamine (10 mg/kg; both Sigma-Aldrich) as described[33,34]. At 15 min after injection, the number of rotations was scored three separate times for 1-min periods, and the average was expressed as the number of full-body turns. Mice selected for transplantation had an average of >10 full-body turns per minute. At 8 weeks after transplantation, mice were perfused transcardially with PBS and then 4% paraformaldehyde. Brains were removed and cryosections were generated at 50-µm thickness. Every fourth section was immunostained for TH using the avidin-biotin peroxidase protocol. After pretreatment with 3% H_2O_2, free-floating sections were incubated sequentially in 1% BSA–0.2% Triton, rabbit antibody to TH (Chemicon), biotinylated anti-rabbit IgG and avidin-biotin-peroxidase complex (Vector). The immunoreaction was visualized using 3,3′-diaminobenzidine tetrahydrochloride dihydrate with nickel intensification (Vector) as the chromogen. The same staining protocol was used on selected sections for GABA, serotonin, GFAP (all Sigma-Aldrich), ChAT (Chemicon), CD11b and CD40 antibodies (both Serotec) using appropriate secondary antibodies. Sections were mounted onto gelatin-coated slides, dehydrated, cleared in xylene and coverslipped. Stereological analysis[35] was carried out for the number of TH-immunoreactive cells (optical fractionator), striatal volume covered by graft (Cavalieri estimator) and TH^+ soma size (nucleator probe) using Stereo Investigator (Version 4.35) (Microbrightfield). Immunohistochemistry for TH-DAT and TH-AADC colocalization was carried out with the same protocol, but using rat DAT (Chemicon) or rabbit AADC (Protos Biotech) antibodies. Sections were incubated in 1% BSA–0.2% Triton X-100 for 30 min, and then in the primary antibody mixture containing rabbit (TH-DAT) or mouse TH (TH/AADC; Sigma-Aldrich) in 0.5% BSA in PBS overnight. Appropriate Cy5 and Cy3 secondary antibodies (Jackson ImmunoResearch) were used for detection.

Statistical analysis. Statistical analyses were carried out using a commercially available software package (Statistica 5.5, Statsoft). Significance of behavioral data was tested by ANOVA (interaction of time × group). Data for the total number of surviving TH^+ cells *in vivo* and neuronal subtype data were tested with ANOVA and Scheffé post hoc analysis. Data are presented as mean ± s.e.m. unless indicated otherwise. All *in vitro* results were derived from at least three independent experiments.

Note: Supplementary information is available on the Nature Biotechnology website.

ACKNOWLEDGMENTS

We thank R. McKay for the Nestin antibody, A. Nagy for the ESB5 cell line, T. Wakayama for the ntES cell lines and E. Lai for the BF1/lacZ ES line. We also thank A. Saxena, P. Song and V. Pratomo for excellent technical assistance, K. Weisel for providing AGM stromal cell lines and R. Stan for a critical review of the manuscript. This work was supported in part by research grants 01.2001.011 and 01.2002.07 from the Michael J. Fox Foundation for Parkinson's Research, and by National Institute of Neurological Disorders and Stroke–National Institutes of Health grant 1R21NS44231-01, as well as by The Parkinson Disease Foundation.

COMPETING INTERESTS STATEMENT

The authors declare that they have no competing financial interests.

Received 7 March 2003; accepted 1 July 2003
Published online at http://www.nature.com/naturebiotechnology/

1. Kawasaki, H. *et al.* Induction of midbrain dopaminergic neurons from ES cells by stromal cell-derived inducing activity. *Neuron* **28**, 31–40 (2000).
2. Lee, S.-H., Lumelsky, N., Studer, L., Auerbach, J.M. & McKay, R.D.G. Efficient generation of midbrain and hindbrain neurons from mouse embryonic stem cells. *Nat. Biotechnol.* **18**, 675–679 (2000).
3. Tropepe, V. *et al.* Direct neural fate specification from embryonic stem cells: a primitive mammalian neural stem cell stage acquired through a default mechanism. *Neuron* **30**, 65–78 (2001).
4. Ying, Q.L., Stavridis, M., Griffiths, D., Li, M. & Smith, A. Conversion of embryonic stem cells into neuroectodermal precursors in adherent monoculture. *Nat. Biotechnol.* **21**, 183–186 (2003).
5. Okabe, S., Forsberg-Nilsson, K., Spiro, A.C., Segal, M. & McKay, R.D.G. Development of neuronal precursor cells and functional postmitotic neurons from embryonic stem cells in vitro. *Mech. Dev.* **59**, 89–102 (1996).
6. Brustle, O. *et al.* Embryonic stem cell–derived glial precursors: a source of myelinating transplants. *Science* **285**, 754–756 (1999).
7. Wakayama, T. *et al.* Differentiation of embryonic stem cell lines generated from adult somatic cells by nuclear transfer. *Science* **292**, 740–743 (2001).
8. Kim, J.H. *et al.* Dopamine neurons derived from embryonic stem cells function in an animal model of Parkinson's disease. *Nature* **418**, 50–56 (2002).
9. Itoh, K. *et al.* Reproducible establishment of hematopoietic supportive stromal cell-lines from murine bone-marrow. *Exp. Hematol.* **17**, 145–153 (1989).
10. Collins, L.S. & Dorshkind, K. A stromal cell-line from myeloid long-term bone-marrow cultures can support myelopoiesis and B-lymphopoiesis. *J. Immunol.* **138**, 1082–1087 (1987).
11. Lendahl, U., Zimmerman, L.B. & McKay, R.D. CNS stem cells express a new class of intermediate filament protein. *Cell* **60**, 585–595 (1990).
12. Sakakibara, S. *et al.* Mouse-Musashi-1, a neural RNA-binding protein highly enriched in the mammalian CNS stem cell. *Dev. Biol.* **176**, 230–242 (1996).
13. Johe, K.K., Hazel, T.G., Müller, T., Dugich-Djordjevic, M.M. & McKay, R.D.G. Single factors direct the differentiation of stem cells from the fetal and adult central nervous system. *Genes Dev.* **10**, 3129–3140 (1996).
14. Studer, L., Tabar, V. & McKay, R.D. Transplantation of expanded mesencephalic precursors leads to recovery in parkinsonian rats. *Nat. Neurosci.* **1**, 290–295 (1998).
15. Yan, J., Studer, L. & McKay, R.D.G. Ascorbic acid increases the yield of dopaminergic

neurons derived from basic fibroblast growth factor–expanded mesencephalic precursors. *J. Neurochem.* **76**, 307–311 (2001).
16. Tao, W. & Lai, E. Telencephalon-restricted expression of BF-1, a new member of the HNF-3/fork head gene family, in the developing rat brain. *Neuron* **8**, 957–966 (1992).
17. Kawasaki, H. *et al.* Generation of dopaminergic neurons and pigmented epithelia from primate ES cells by stromal cell–derived inducing activity. *Proc. Natl. Acad. Sci. USA* **99**, 1580–1585 (2002).
18. Cibelli, J.B. *et al.* Parthenogenetic stem cells in nonhuman primates. *Science* **295**, 819 (2002).
19. Wichterle, H., Lieberam, I., Porter, J.A. & Jessell, T.M. Directed differentiation of embryonic stem cells into motor neurons. *Cell* **110**, 385–397 (2002).
20. Munoz-Sanjuan, I. & Brivanlou, A.H. Neural induction, the default model and embryonic stem cells. *Nat. Rev. Neurosci.* **3**, 271–280 (2002).
21. Lumsden, A. & Krumlauf, R. Patterning the vertebrate neuraxis (Review). *Science* **274**, 1109–1115 (1996).
22. Wilson, S.W. & Rubenstein, J.L.R. Induction and dorsoventral patterning of the telencephalon. *Neuron* **28**, 641–651 (2000).
23. Sanchez-Pernaute, R., Studer, L., Bankiewicz, K.S., Major, E.O. & McKay, R.D. *In vitro* generation and transplantation of precursor-derived human dopamine neurons. *J. Neurosci. Res.* **65**, 284–288 (2001).
24. Ling, Z.D., Potter, E.D., Lipton, J.W. & Carvey, P.M. Differentiation of mesencephalic progenitor cells into dopaminergic neurons by cytokines. *Exp. Neurol.* **149**, 411–423 (1998).
25. Wagner, J. *et al.* Induction of a midbrain dopaminergic phenotype in Nurr1-overexpressing neural stem cells by type 1 astrocytes. *Nat. Biotechnol.* **17**, 653–659 (1999).
26. Bjorklund, L.M. *et al.* Embryonic stem cells develop into functional dopaminergic neurons after transplantation in a Parkinson rat model. *Proc. Natl. Acad. Sci. USA* **99**, 2344–2349 (2002).
27. Zawada, W.M. *et al.* Somatic cell cloned transgenic bovine neurons for transplantation in parkinsonian rats. *Nat. Med.* **4**, 569–574 (1998).
28. Xuan, S. *et al.* Winged helix transcription factor BF-1 is essential for the development of the cerebral hemispheres. *Neuron* **14**, 1141–1152 (1995).
29. Keller, G.M. *In-vitro* differentiation of embryonic stem-cells. *Curr. Opin. Cell Biol.* **7**, 862–869 (1995).
30. Xu, M.J. *et al.* Stimulation of mouse and human primitive hematopoiesis by murine embryonic aorta-gonad-mesonephros-derived stromal cell lines. *Blood* **92**, 2032–2040 (1998).
31. Studer, L. *et al.* Noninvasive dopamine determination by reversed phase HPLC in the medium of free-floating roller tube cultures of rat fetal ventral mesencephalon: a tool to assess dopaminergic tissue prior to grafting. *Brain Res. Bull.* **41**, 143–150 (1996).
32. Battisti, J.J., Uretsky, N.J. & Wallace, L.J. Sensitization of apomorphine-induced stereotyped behavior in mice is context dependent. *Psychopharmacology (Berl.)* **146**, 42–48 (1999).
33. Winkler, J.D. & Weiss, B. Reversal of supersensitive apomorphine-induced rotational behavior in mice by continuous exposure to apomorphine. *J. Pharmacol. Exp. Ther.* **238**, 242–247 (1996).
34. Barneoud, P. *et al.* Effects of complete and partial lesions of the dopaminergic mesotelencephalic system on skilled forelimb use in the rat. *Neuroscience* **67**, 837–848 (1995).
35. Gundersen, H.J.G. *et al.* Some new, simple and efficient stereological methods and their use in pathological research and diagnosis. *APMIS* **96**, 379–394 (1988).